

Magnetic and superconducting transitions in $\text{Ba}_{1-x}\text{K}_x\text{Fe}_2\text{As}_2$ studied by specific heat

Ch. Kant, J. Deisenhofer,* A. Günther, F. Schrettle, and A. Loidl
*Experimentalphysik V, Center for Electronic Correlations and Magnetism,
Institute for Physics, Augsburg University, D-86135 Augsburg, Germany*

M. Rotter and D. Johrendt
*Department Chemie und Biochemie, Ludwig-Maximilians-Universität München,
Butenandtstrasse 5-13 (Haus D), 81377 München, Germany*

(Dated: September 16, 2018)

We report on specific heat measurements in $\text{Ba}_{1-x}\text{K}_x\text{Fe}_2\text{As}_2$ ($x \leq 0.6$). For the underdoped sample with $x = 0.2$ both the spin-density-wave transition at $T = 100$ K and the superconducting transition at 23 K can be identified. The electronic contribution to the specific heat in the superconducting state for concentrations in the vicinity of optimal doping $x = 0.4$ can be well described by a full single-gap within the BCS limit.

PACS numbers: 74.25.Bt, 74.25.Fy, 75.30.Fv

Since the discovery of superconductivity in Fe-based pnictides,^{1,2} the superconducting (SC) transition temperature could be raised from $T_c = 27$ K to a maximum of 55 K in the so-called 1111-systems $R\text{FeAsO}$ ($R = \text{La} - \text{Gd}$).³ Subsequently, further classes of SC compounds containing FeAs layers were reported: the 122-systems $A\text{Fe}_2\text{As}_2$ with $A = \text{Ba}, \text{Sr}, \text{Ca}, \text{Eu}$ and a T_c up to 38 K,^{4,5,6,7} the 111-compounds LiFeAs and NaFeAs ^{8,9} and the binary chalcogenide systems like Fe_{1+x}Se .^{10,11,12} Recently, compounds where the superconducting FeAs layers are separated by conducting transition-metal oxide blocks were reported with $T_c = 37$ K.^{13,14,15} In the first two material classes, the mother parent compounds undergo a transition from a poorly metallic state with tetragonal symmetry to a spin-density wave (SDW) low-temperature state with orthorhombic distortions.^{16,17,18} The SC state in the 122 compounds can be reached, e.g., by substituting the A -site ions by K ^{4,5} or doping the FeAs layers with Co .^{6,7}

One exciting and controversial issue is the competition or coexistence of magnetism and superconductivity in the underdoped concentration regimes and the relation to the structural distortions. While in the 1111-systems magnetism seems to be completely suppressed before superconductivity appears,¹⁹ in $\text{Ba}_{1-x}\text{K}_x\text{Fe}_2\text{As}_2$ the coexistence of orthorhombic distortions and superconductivity has been reported up to $x \approx 0.2$ ($T_c \approx 26$ K),^{17,18} and the persistence of long-range antiferromagnetic ordering up to $x = 0.3$.²⁰ Several local-probe studies like μSR found evidence for a phase separation into SC and antiferromagnetic domains.^{21,22,23} Recent neutron scattering studies on lightly Co doped BaFe_2As_2 revealed that the structural and antiferromagnetic transition do not occur concomitantly for $x > 0$ and that for $x = 0.047$ both an AFM and a SC transition are present.^{24,25}

The symmetry of the SC order parameter is another important question under discussion: A growing number of theoretical and experimental studies seem to be consistent with theoretically suggested s^\pm -wave model^{26,27} with a sign reversal between the two Fermi surfaces. How-

ever, the existence of line nodes has not been clarified yet. For example, nuclear magnetic resonance or thermal conductivity studies report both evidence for a fully gapped state^{28,29} and for nodal lines.^{30,31,32,33} ARPES measurements revealed again nearly isotropic and nodeless gaps.^{34,35,36,37} This controversy seems to be related to the effects of doping,³⁸ which is in agreement with the findings in $\text{Ba}_{1-x}\text{K}_x\text{Fe}_2\text{As}_2$, where a fully gapped state seems to exist for $x \simeq 0.3$,²⁹ but KFe_2As_2 reportedly exhibits line nodes.^{33,39}

Specific heat measurements provide clear signatures of the antiferromagnetic and SC phase transitions and are sensitive to the symmetry of the SC order parameter, which determines the electronic part of the specific heat below T_c . The specific heat of several samples with a nominal composition in the vicinity of the optimal doping $x = 0.4$ have been reported previously^{16,18,40,41,42} and it became clear that a major difficulty consists in modeling the normal state contribution to the specific heat.⁴³ Hence, most studies focused on the evaluation of the jump in C/T at the superconducting transition.^{16,18,40,41,43} Mu *et al.* extracted the electronic specific heat in the SC state and fitted the data using s -wave isotropic BCS theory with a single gap $\Delta = 6$ meV⁴² in agreement with the low-energy gaps reported by other experimental techniques like optical spectroscopy and ARPES (see e.g. Ref. 44 and references therein).

In this work we report on the specific heat of polycrystalline $\text{Ba}_{1-x}\text{K}_x\text{Fe}_2\text{As}_2$ for $x \leq 0.6$. A part of the data was presented without a detailed analysis already in Ref. 18. We model the normal-state contribution of the specific heat to access the anomalies at the SC and magnetic phase transitions. For $x = 0.2$ we observe a strongly broadened SDW anomaly and a superconducting transition at about 23 K. Concerning the symmetry of the SC order parameter we find that the electronic part of the specific heat in the SC state around the optimal doping $x = 0.4$ is well described by using a single gap.

Polycrystalline samples of $\text{Ba}_{1-x}\text{K}_x\text{Fe}_2\text{As}_2$ with $x = 0.0, 0.1, 0.2, 0.3, 0.5$, and 0.6 were prepared as described

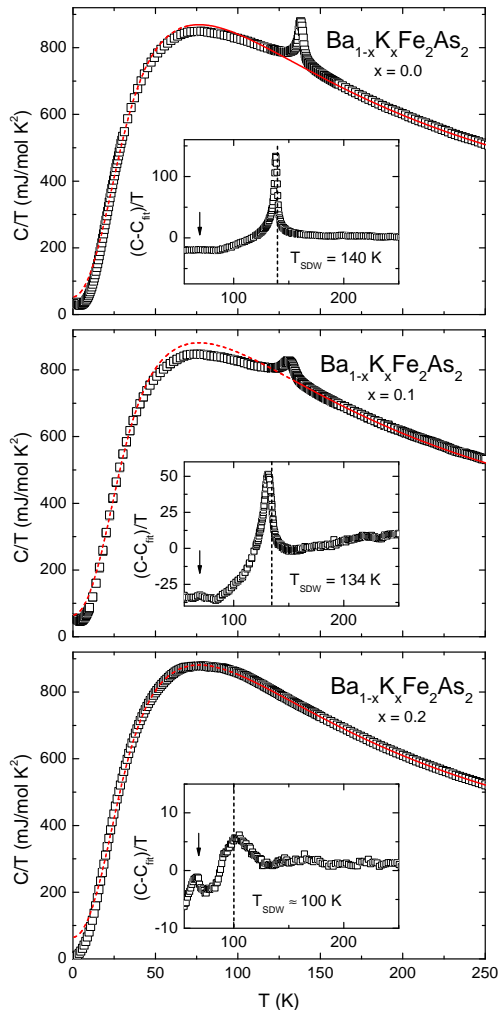


FIG. 1: (color online) C/T vs. T of $\text{Ba}_{1-x}\text{K}_x\text{Fe}_2\text{As}_2$ for $x \leq 0.2$. The lines are fits to the data of the high temperature structure (see text). Insets: Residual heat after subtracting the model from the experimental data. Arrows indicate contributions assigned to FeAs.

in Refs. 17,18 and characterized by X-ray powder diffraction and resistivity measurements. The magnetic properties were studied using a commercial SQUID magnetometer (Quantum Design MPMS-5) with external magnetic fields up to 50 kOe. The heat capacity was measured in a Quantum Design Physical Properties Measurement System for temperatures from $2 \text{ K} < T < 300 \text{ K}$.

The main frames of Fig. 1 show the specific heat divided by temperature C/T of the samples with $x \leq 0.2$. Anomalies attributed to the reported SDW transition can be identified at 140 K and 134 K for $x = 0$ and $x = 0.1$, respectively. In the case of $x = 0.2$, however, only an extremely broadened and weak feature at around 100 K can be presumed, although a structural transition was clearly identified to occur in this temperature range.¹⁸ Similarly, susceptibility measurements showed bulk superconduc-

tivity in this sample below 23 K, while no evident feature was discernible in C/T at this temperature.¹⁸ To reveal the SDW and superconducting transitions, we model the specific heat above the corresponding SDW and superconducting transitions by

$$C(T) = D(\theta_D, T) + 2E(\theta_{E1}, T) + 2E(\theta_{E2}, T) + \gamma T \quad (1)$$

where D and E denote isotropic Debye and Einstein contributions with the corresponding Debye and Einstein temperatures θ_D , θ_{E1} , and θ_{E2} and γ is the Sommerfeld coefficient. The ratios were kept fixed for all investigated samples to comply with the lattice degrees of freedom. We started out with the sample with $x = 0.3$, because at this concentration no structural or magnetic transitions seem to occur and the system remains tetragonal down to lowest temperatures.¹⁸ The parameters obtained for $\text{Ba}_{0.7}\text{K}_{0.3}\text{Fe}_2\text{As}_2$ were then slightly adapted to describe the specific heat in the tetragonal phase for the samples with $x \leq 0.2$. The resulting curves reproduce the data nicely in the tetragonal phase and are shown as solid lines in Fig. 1 for $T \geq T_{SDW}$ and the extrapolations for $T < T_{SDW}$ are shown as dashed lines. The obtained fit parameters are listed in Tab. I.

The data after subtraction of the modeled normal-state contribution $(C - C_{fit})/T$ is shown in the corresponding insets of Fig. 1. Immediately, one recognizes the sharp SDW transitions for $x = 0.0$ and $x = 0.1$. For $x = 0.2$ a strongly broadened anomaly at around 100 K now becomes clearly visible, in agreement with the observed SDW anomalies in the resistivity and the structural transition.¹⁸ The weak features visible at about 70 K and present in all three samples are probably traces of binary FeAs, which reportedly orders helimagnetically in this temperature range.⁴⁵ Hence, subtracting the modeled normal-state contribution allows to reveal the SDW transition anomalies, but the validity of this modelling is naturally limited by the electronic reconstruction, the possible contributions of magnetic excitations, and the structural changes occurring at the SDW transition.

Therefore, we follow a different route to uncover the SC transition in the $x = 0.2$ sample which was revealed by susceptibility measurements to occur at about 23 K.¹⁸ We used the data for the pure BaFe_2As_2 as a refer-

TABLE I: Fit parameters for the specific heat of $\text{Ba}_{1-x}\text{K}_x\text{Fe}_2\text{As}_2$ at various doping levels using Eq. 1.

x	θ_D/K	θ_{E1}/K	θ_{E2}/K	$\gamma/\frac{\text{mJ}}{\text{mol K}^2}$
0.0	144	183	365	53
0.1	144	183	365	65
0.2	144	183	365	65
0.3	144	183	365	53
0.4	144	185	378	49
0.5	145	186	374	54
0.6	155	188	359	58

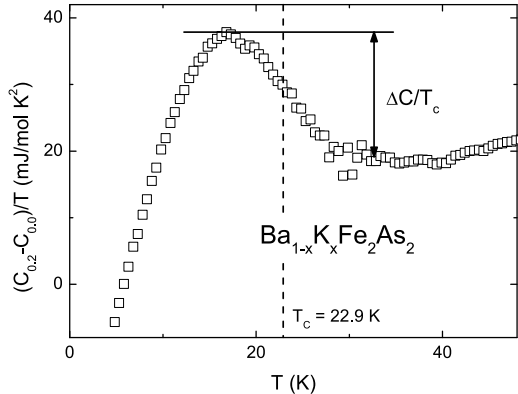


FIG. 2: Difference of the specific heat for $x = 0.2$ and $x = 0.0$ divided by temperature.

ence for a system in the SDW state state but without superconductivity at low temperatures. Moreover, the normal-state parameters for both compounds are very similar. The resulting low-temperature electronic specific heat is shown in Fig. 2. A clear anomaly with a midpoint temperature of $T_c = 22.9$ K and a jump $\Delta C/T_c = 19.2$ mJ/molK² is in good agreement with the SC transition temperature determined from susceptibility measurements.¹⁸ We would like to emphasize that both the SDW transition and the SC anomaly are very broad and indicate a distribution of the corresponding transition temperatures. We interpret both features as due to strong magnetic and SC fluctuations similarly to the results reported for Co doped BaFe₂As₂.^{24,25}

Having discussed the data for the samples which exhibit a SDW transition, we now turn to the samples where magnetic ordering and orthorhombic distortions are absent and the structure remains tetragonal down to lowest temperatures: The main frames in Fig. 3 show C/T vs. T of Ba_{1-x}K_xFe₂As₂ for $x = 0.3$, 0.4, and 0.5. The transitions into the superconducting states are clearly visible as peaks in the experimental data for all three compounds. Again, the lines are the modeled electronic and lattice contributions of the normal state according to Eq. (1) using the parameters given in Tab. I. The model reproduces the data above T_c nicely.

The electronic part obtained by subtracting the modeled normal-state contribution is shown in the corresponding insets. The residual electronic specific heat C_{el} can be well described by the BCS derived α -model:^{46,47}

$$C_{el} = T \frac{dS_{el}}{dT} \quad (2)$$

$$S_{el} = -\frac{6\gamma}{\pi^2 k_B} \int_0^{\infty} d\epsilon (f \ln f + (1-f) \ln(1-f)) \quad (3)$$

Here, the ratio of the energy gap Δ_0 at 0 K and T_c is not fixed ($2\Delta_0/k_B T_c = 3.53$ in the BCS theory) but left

as a free fitting parameter. The Fermi-Dirac distribution $f = f(E, T) = [\exp(E/k_B T) + 1]^{-1}$ is determined by the energy $E = \sqrt{\epsilon^2 + \Delta^2(T)}$, where ϵ denotes the energy of independent fermion quasiparticles measured relative to the Fermi surface. The temperature dependence of the gap $\Delta(T) = \Delta_0 \delta(T/T_c)$ is assumed to be the same as calculated by Mühlischlegel,⁴⁸ where δ is the normalized BCS gap in the limit of weak-coupling superconductors. The obtained fit curves are shown as solid lines in the

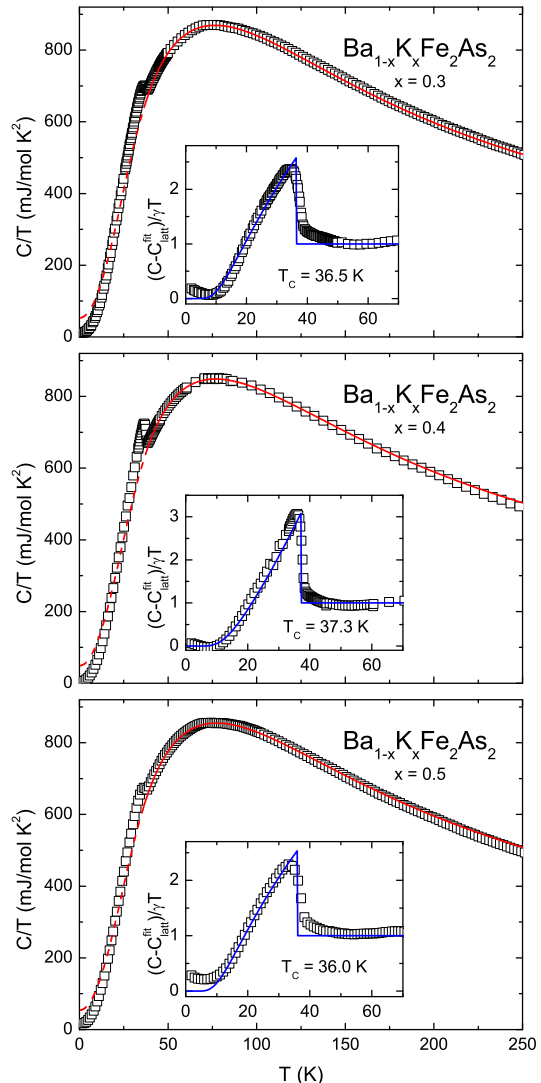


FIG. 3: (Color online) Temperature dependence of C/T of Ba_{1-x}K_xFe₂As₂ for $x = 0.3$, 0.4, and 0.5. The lines in the main frames are fits using Eq. (1) in the normal conducting state. Extrapolation of the fits to lower temperature are dashed. The insets show the difference between C/T and the modeled phonon contribution normalized by the normal-state Sommerfeld coefficient γ together with a fit according to Eqs. (2) and (3).

TABLE II: Parameters determining the electronic specific heat for $\text{Ba}_{1-x}\text{K}_x\text{Fe}_2\text{As}_2$ according to the model described in the text.

	$x = 0.3$	$x = 0.4$	$x = 0.5$
T_c / K	36.5	37.3	36.0
Δ_0 / K	68	78	66
$2\Delta_0/k_B T_c$	3.73	4.14	3.67

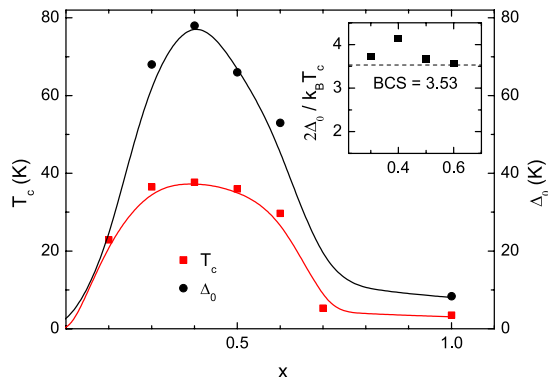


FIG. 4: (Color online) Critical temperatures and SC gaps plotted vs. doping level x . Lines are drawn to guide the eye. Data for $x = 1.0$ is taken from Ref. 39. Inset: Coupling parameters $2\Delta_0/T_c$ vs. x compared to the BCS value of 3.53.

insets of Fig. 3.

For the Sommerfeld coefficient γ we fixed the value to the parameters given in Tab. I for the normal state. The above model leads to the fit parameters presented in Tab. II. As expected the optimally doped sample

with $x = 0.4$ exhibits the highest values for $T_c = 37.3$ K and $\Delta_0 = 78$ K. The critical temperatures for the compounds with $x = 0.3$ and $x = 0.5$ are close to this optimal value, but the zero temperature gaps are already reduced (Fig. 4). The coupling parameters $2\Delta_0/T_c$ are in good agreement with the BCS value of 3.53. For the sample with $x = 0.4$, the ratio $2\Delta_0/T_c = 4.14$ is enhanced signaling stronger coupling (see inset of Fig. 4). The corresponding gap value $\Delta_0 = 6.7$ meV is in good agreement with the 6 meV derived by Mu *et al.* from specific heat and corresponds to the small-gap value observed also by ARPES, optical spectroscopy, and other techniques (for an overview see e.g. Ref. 44 and references therein). Since the transport properties within the suggested s^\pm symmetry can be considered the same as for a conventional two-gap superconductor,²⁶ we also tried to describe our data using two gap parameters. However, this procedure did not yield a significant improvement of the fit and, therefore, we conclude that the electronic part of the specific heat is dominated by the low-energy superconducting gap without nodes.

In summary, our specific heat measurements revealed the existence of two phase transitions for the sample with $x = 0.2$, a broad transition at about 100 K associated with magnetic ordering and a broad anomaly at transition to the superconducting ground state at 23 K. Moreover, the electronic part of the specific heat of $\text{Ba}_{1-x}\text{K}_x\text{Fe}_2\text{As}_2$ in the vicinity of optimal doping ($0.3 \leq x \leq 0.6$) could be well described by the phenomenological α -model for a s -type superconductor with a single full gap and coupling parameters $2\Delta_0/T_c$ close to the weak-coupling BCS limit.

We thank S. Graser and E.W. Scheidt for fruitful discussions. The work was supported partially by the DFG via SFB 484.

* Electronic address: joachim.deisenhofer@physik.uni-augsburg.de⁹

¹ Y. Kamihara, T. Watanabe, M. Hirano, and H. Hosono, J. Am. Chem. Soc. **130**, 3296 (2008).
² X. H. Chen, T. Wu, G. Wu, R. H. Liu, H. Chen, and D. F. Fang, Nature **453**, 761 (2008).
³ Z.-A. Ren, W. Lu, J. Zang, W. Yi, X.-L. Shen, Z.-C. Li, G.-C. Che, D. Xiao-Li, L.-L. Sun, F. Zhou, et al., Chin. Phys. Lett. **25**, 2215 (2008).
⁴ M. Rotter, M. Tegel, and D. Johrendt, Phys. Rev. Lett. **101**, 107006 (2008).
⁵ H. S. Jeevan, Z. Hossain, D. Kasinathan, H. Rosner, C. Geibel, and P. Gegenwart, Phys. Rev. B **78**, 092406 (2008).
⁶ A. S. Sefat, R. Jin, M. A. McGuire, B. C. Sales, D. J. Singh, and D. Mandrus, Phys. Rev. Lett. **101** (2008).
⁷ A. Leithe-Jasper, W. Schnelle, C. Geibel, and H. Rosner, Phys. Rev. Lett. **101**, 207004 (2008).
⁸ J. H. Tapp, Z. Tang, B. Lv, K. Sasmal, B. Lorenz, P. C. W. Chu, and A. M. Guloy, Phys. Rev. B **78**, 060505(R) (2008).

D. R. Parker, M. J. Pitcher, P. J. Baker, I. Franke, T. Lancaster, S. J. Blundell, and S. J. Clarke, Chem. Commun. p. 2189 (2009).
¹⁰ F.-C. Hsu, J.-Y. Luo, K.-W. Yeh, T.-K. Chen, T.-W. Huang, P. M. Wu, Y.-C. Lee, Y.-L. Huang, Y.-Y. Chu, D.-C. Yan, et al., Proc. Natl. Acad. Sci. U.S.A. **105**, 14262 (2008).
¹¹ Y. Mizuguchi, F. Tomioka, S. Tsuda, T. Yamaguchi, and Y. Takano, Appl. Phys. Lett. **93**, 152505 (2008).
¹² S. Medvedev, T. M. McQueen, I. A. Troyan, T. Palasyuk, M. I. Erements, R. J. Cava, S. Naghavi, F. Casper, V. Ksenofontov, G. Wortmann, et al., Nature Mater. **8**, 630 (2009).
¹³ H. Ogino, Y. Matsumura, Y. Katsura, K. Ushiyama, S. Horii, K. Kishio, and J.-i. Shimoyama, Supercond. Sci. Technol. **22**, 075008 (2009).
¹⁴ Y. L. Xie, R. H. Liu, T. Wu, G. Wu, Y. A. Song, D. Tan, W. X. F., H. Chen, J. J. Ying, Y. J. Yang, et al., Europhys. Lett. **86** (2009).

- ¹⁵ X. Zhu, F. Han, G. Mu, P. Cheng, B. Shen, B. Zeng, and H.-H. Wen, *Phys. Rev. B* **79** (2009).
- ¹⁶ J. K. Dong, L. Ding, H. Wang, X. F. Wang, T. Wu, G. Wu, X. H. Chen, and S. Y. Li, *New J. Phys.* **10**, 123031 (2008).
- ¹⁷ M. Rotter, M. Pangerl, M. Tegel, and D. Johrendt, *Angew. Chem. Int. Ed.* **47**, 7949 (2008).
- ¹⁸ M. Rotter, M. Tegel, I. Schellenberg, F. M. Schappacher, R. Pöttgen, J. Deisenhofer, A. Günther, F. Schrettle, A. Loidl, and D. Johrendt, *New. J. Phys.* **11**, 025014 (2009).
- ¹⁹ C. de la Cruz, Q. Huang, J. W. Lynn, J. Li, I. Ratcliff, W., J. L. Zarestky, H. A. Mook, G. F. Chen, J. L. Luo, N. L. Wang, et al., *Nature* **453**, 899 (2008).
- ²⁰ H. Chen, Y. Ren, Y. Qiu, W. Bao, R. H. Liu, G. Wu, T. Wu, Y. L. Xie, X. F. Wang, Q. Huang, et al., *Europhys. Lett.* **85**, 17006 (2009).
- ²¹ A. A. Aczel, E. Baggio-Saitovitch, S. L. Budko, P. C. Canfield, J. P. Carlo, G. F. Chen, P. Dai, T. Goko, W. Z. Hu, G. M. Luke, et al., *Phys. Rev. B* **78**, 214503 (2008).
- ²² T. Goko, A. A. Aczel, E. Baggio-Saitovitch, S. L. Bud'ko, P. C. Canfield, J. P. Carlo, G. F. Chen, P. Dai, A. C. Hamann, W. Z. Hu, et al., *Phys. Rev. B* **80**, 024508 (2009).
- ²³ J. T. Park, D. S. Inosov, C. Niedermayer, G. L. Sun, D. Haug, N. B. Christensen, R. Dinnebier, A. V. Boris, A. J. Drew, L. Schulz, et al., *Phys. Rev. Lett.* **102** (2009).
- ²⁴ D. K. Pratt, W. Tian, A. Kreyssig, J. L. Zarestky, S. Nandi, N. Ni, S. L. Bud'ko, P. C. Canfield, A. I. Goldman, and R. J. McQueeney, *Phys. Rev. Lett.* **103**, 087001 (2009).
- ²⁵ A. D. Christianson, M. D. Lumsden, S. E. Nagler, G. J. MacDougall, M. A. McGuire, A. S. Sefat, R. Jin, B. C. Sales, and D. Mandrus, *Phys. Rev. Lett.* **103**, 087002 (2009).
- ²⁶ I. I. Mazin, D. J. Singh, M. D. Johannes, and M. H. Du, *Phys. Rev. Lett.* **101**, 057003 (2008).
- ²⁷ A. V. Chubukov, D. V. Efremov, and I. Eremin, *Phys. Rev. B* **78**, 134512 (2008).
- ²⁸ M. Yashima, H. Nishimura, H. Mukuda, Y. Kitaoka, K. Miyazawa, P. M. Shirage, K. Kiho, H. Kito, H. Eisaki, and A. Iyo, arXiv:0905.1896v1 (unpublished).
- ²⁹ X. G. Luo, M. A. Tanatar, J.-P. Reid, H. Shakeripour, N. Doiron-Leyraud, N. Ni, S. L. Bud'ko, P. C. Canfield, H. Luo, Z. Wang, et al., arXiv:0904.4049v1 (unpublished).
- ³⁰ Y. Nakai, K. Ishida, Y. Kamihara, M. Hirano, and H. Hosono, *J. Phys. Soc. Jpn.* **77**, 073701 (2008).
- ³¹ H. J. Grafe, D. Paar, G. Lang, N. J. Curro, G. Behr, J. Werner, J. Hamann-Borrero, C. Hess, N. Leps, R. Klingeler, et al., *Phys. Rev. Lett.* **101**, 047003 (2008).
- ³² H. Mukuda, N. Terasaki, H. Kinouchi, M. Yashima, Y. Kitaoka, S. Suzuki, S. Miyasaka, S. Tajima, K. Miyazawa, P. Shirage, et al., *J. Phys. Soc. Jpn.* **77**, 093704 (2008).
- ³³ J. K. Dong, S. Y. Zhou, T. Y. Guan, H. Zhang, Y. F. Dai, X. Qiu, X. F. Wang, Y. He, X. H. Chen, and S. Y. Li, arXiv:0909.4855 (unpublished).
- ³⁴ H. Luetkens, H. H. Klauss, R. Khasanov, A. Amato, R. Klingeler, I. Hellmann, N. Leps, A. Kondrat, C. Hess, A. Koehler, et al., *Phys. Rev. Lett.* **101**, 097009 (2008).
- ³⁵ K. Hashimoto, T. Shibauchi, T. Kato, K. Ikada, R. Okazaki, H. Shishido, M. Ishikado, H. Kito, A. Iyo, H. Eisaki, et al., *Phys. Rev. Lett.* **102**, 017002 (2009).
- ³⁶ T. Kondo, A. F. Santander-Syro, O. Copie, C. Liu, M. E. Tillman, E. D. Mun, J. Schmalian, S. L. Bud'ko, M. A. Tanatar, P. C. Canfield, et al., *Phys. Rev. Lett.* **101**, 147003 (2008).
- ³⁷ H. Ding, P. Richard, K. Nakayama, K. Sugawara, T. Arakane, Y. Sekiba, A. Takayama, S. Souma, T. Sato, T. Takahashi, et al., *Europhys. Lett.* **83**, 47001 (2008).
- ³⁸ K. Kuroki, H. Usui, S. Onari, R. Arita, and H. Aoki, *Phys. Rev. B* **79**, 224511 (2009).
- ³⁹ H. Fukazawa, Y. Yamada, K. Kondo, T. Saito, Y. Kohori, K. Kuga, Y. Matsumoto, S. Nakatsuji, H. Kito, P. Shirage, et al., arXiv:0906.4644v1 (unpublished).
- ⁴⁰ N. Ni, S. L. Bud'ko, A. Kreyssig, S. Nandi, G. E. Rustan, A. I. Goldman, S. Gupta, J. D. Corbett, A. Kracher, and P. C. Canfield, *Phys. Rev. B* **78**, 014507 (2008).
- ⁴¹ U. Welp, R. Xie, A. E. Koshelev, W. K. Kwok, H. Q. Luo, Z. S. Wang, G. Mu, and H. H. Wen, *Phys. Rev. B* **79**, 094505 (2009).
- ⁴² G. Mu, H. Luo, Z. Wang, L. Shan, C. Ren, and H.-H. Wen, *Phys. Rev. B* **79**, 174501 (2009).
- ⁴³ S. L. Bud'ko, N. Ni, and P. C. Canfield, *Phys. Rev. B* **79**, 220516(R) (2009).
- ⁴⁴ D. V. Evtushinsky, D. S. Inosov, V. B. Zabolotnyy, M. S. Viazovska, R. Khasanov, A. Amato, H.-H. Klauss, H. Luetkens, C. Niedermayer, G. L. Sun, et al., *New J. Phys.* **11**, 055069 (2009).
- ⁴⁵ D. Gonzalez-Alvarez, F. Grønsvold, B. Falk, E. F. Westrum, Jr., R. Blachnik, and G. Kudermand, *J. Chem. Thermodyn.* **21**, 363 (1989).
- ⁴⁶ F. Bouquet, Y. Wang, R. A. Fisher, D. G. Hinks, J. D. Jorgensen, A. Junod, and N. E. Phillips, *Europhys. Lett.* **56**, 856 (2001).
- ⁴⁷ H. Padamsee, J. E. Neighbor, and C. A. Shiffman, *J. Low Temp. Phys.* **12**, 387 (1973).
- ⁴⁸ B. Mühlischlegel, *Z. Phys.* **155**, 313 (1959).